

**Electronic Supplementary Information**

**Transmetallation of Bis(6-diphenylphosphinoxy-acenaphth-5-yl)mercury with  
Tin Tetrachloride, Antimony Trichloride and Bismuth Trichloride**

Marian Olaru,<sup>a</sup> Sandra Krupke,<sup>a</sup> Enno Lork,<sup>a</sup> Stefan Mebs,<sup>\*b</sup> Jens Beckmann<sup>\*a</sup>

<sup>a</sup> *Institut für Anorganische Chemie und Kristallographie, Universität Bremen, Leobener Straße 7,  
28359 Bremen, Germany*

<sup>b</sup> *Institut für Experimentalphysik, Freie Universität Berlin, Arnimallee 14, 14195 Berlin, Germany*

---

<sup>\*</sup> Correspondence to Jens Beckmann (E-mail: [j.beckmann@uni-bremen.de](mailto:j.beckmann@uni-bremen.de)) and Stefan Mebs (E-mail: [stebs@chemie.fu-berlin.de](mailto:stebs@chemie.fu-berlin.de))

## **Contents**

NMR spectra.....	2
Computational data.....	12
Crystallographic data.....	18

## NMR spectra

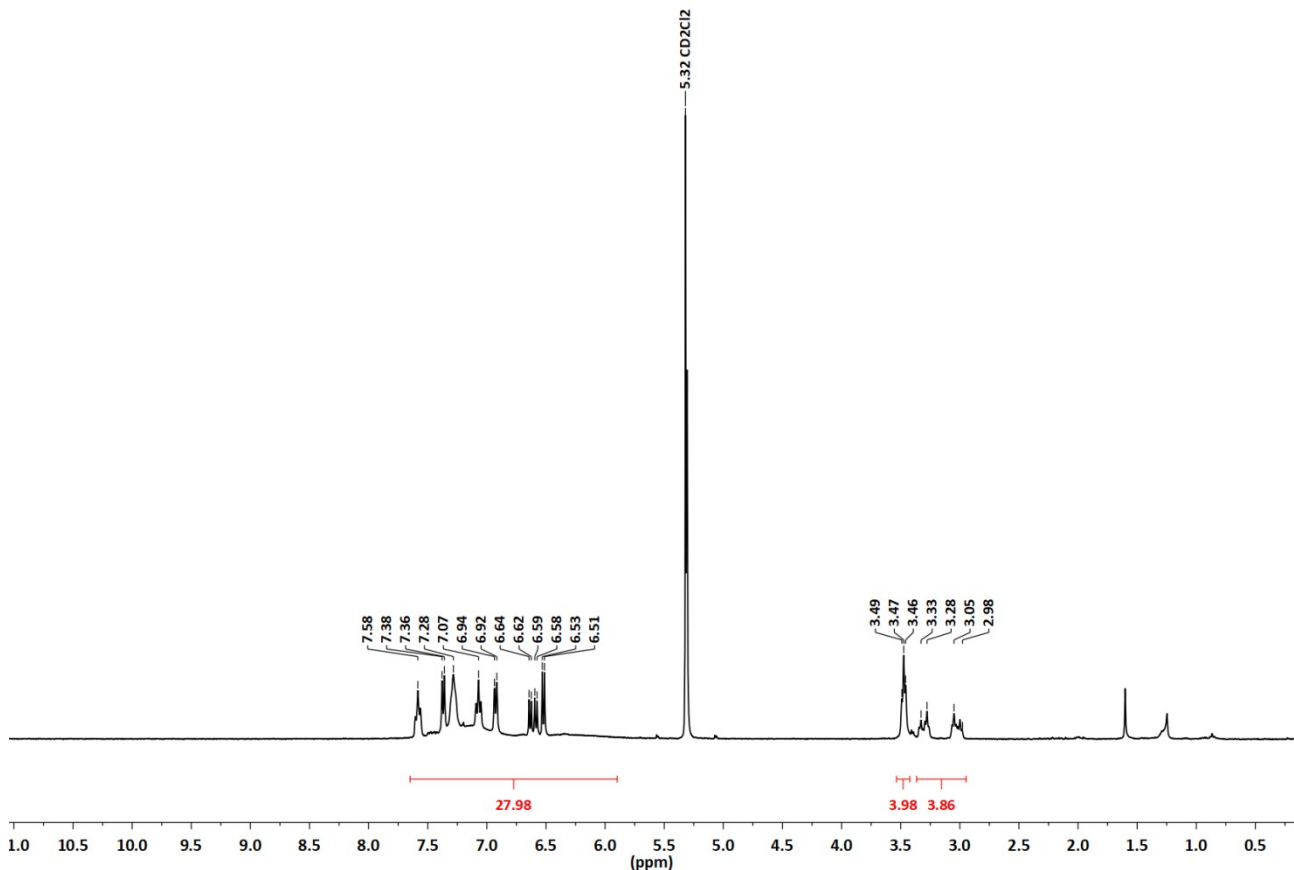


**Figure S1.** <sup>1</sup>H NMR (360 MHz, CD<sub>2</sub>Cl<sub>2</sub>) spectrum of **1a**.

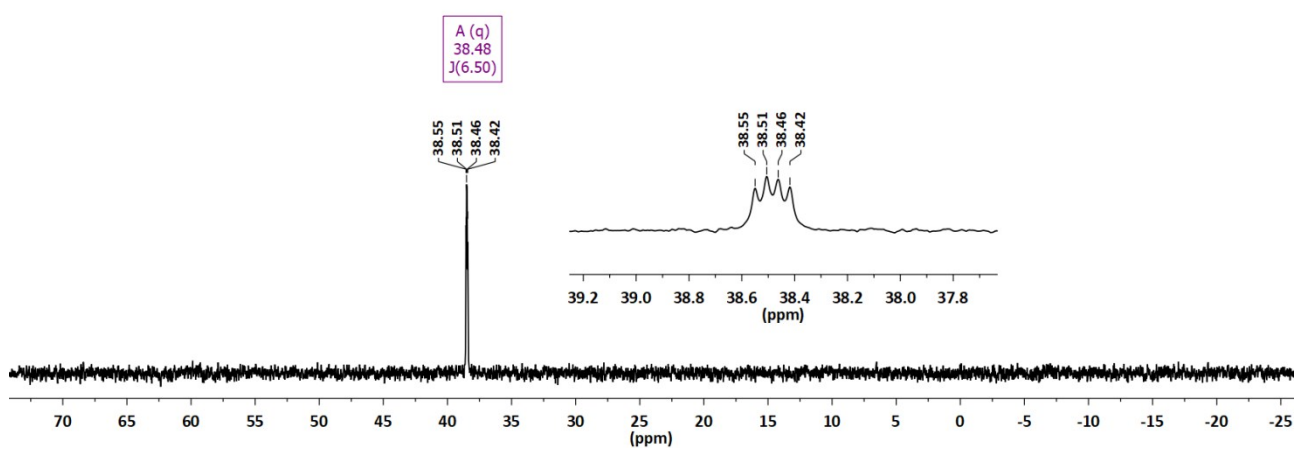


**Figure S2.** <sup>31</sup>P NMR (146 MHz, CD<sub>2</sub>Cl<sub>2</sub>) spectrum of **1a**.

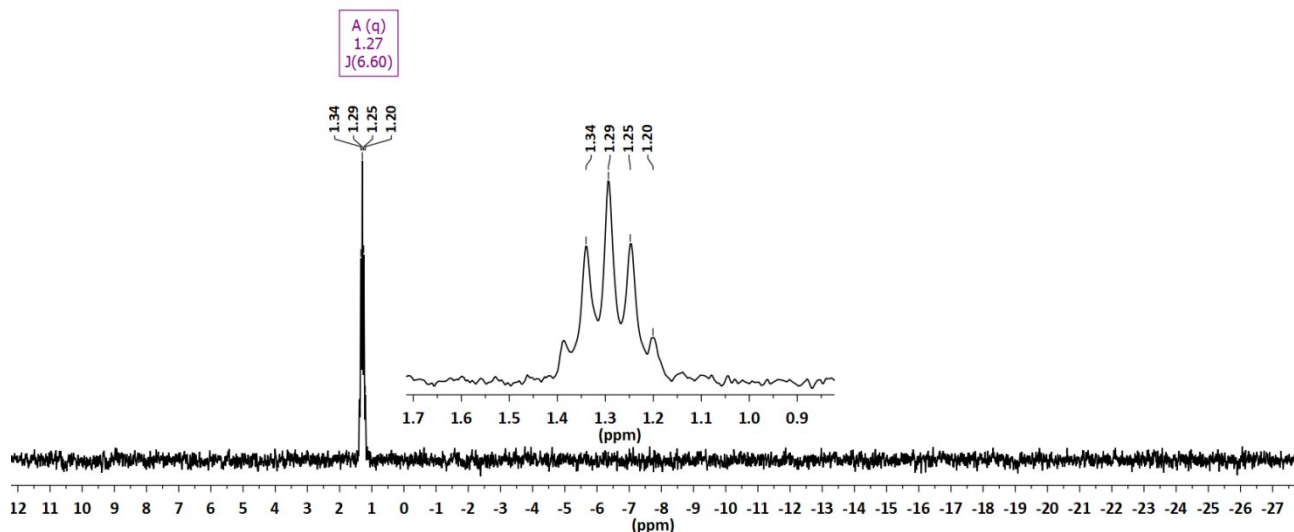


**Figure S3.**  $^7\text{Li}$  NMR (140 MHz,  $\text{CD}_2\text{Cl}_2$ ) spectrum of **1a**.

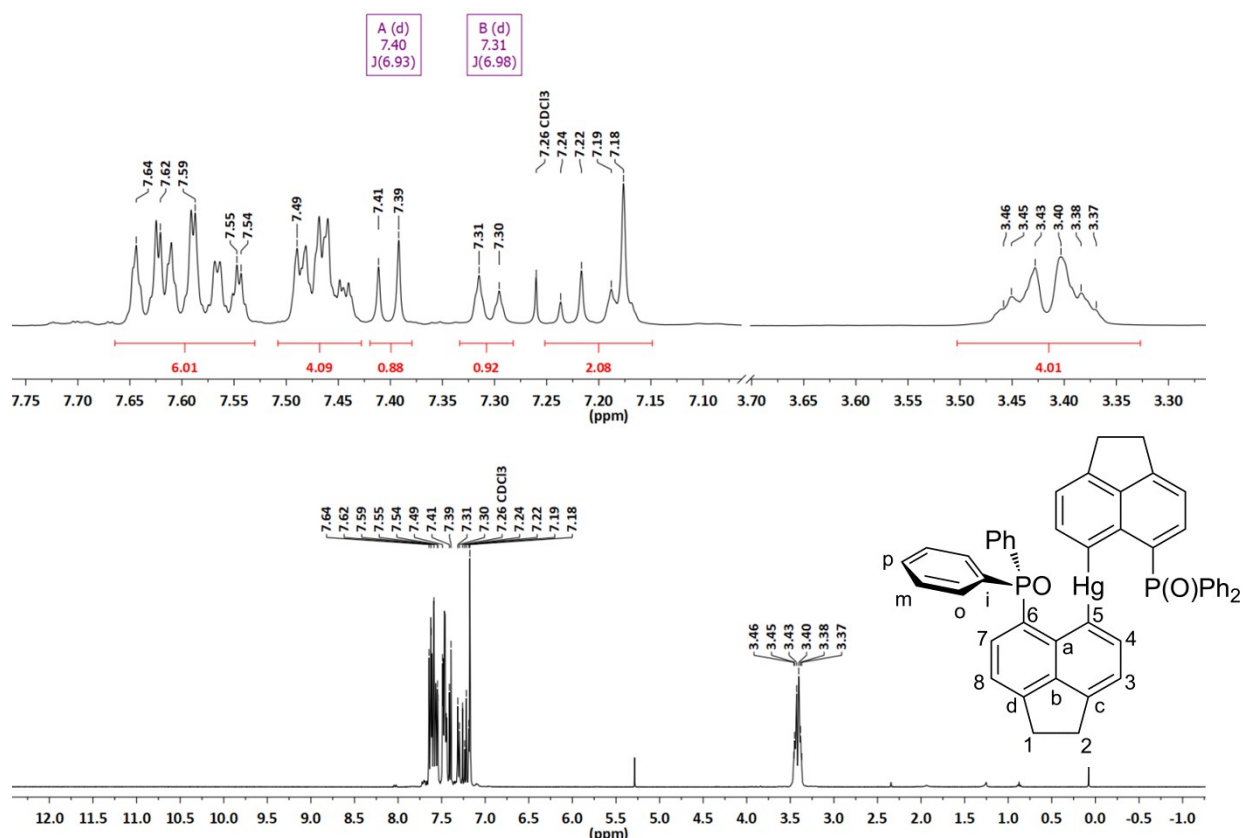


**Figure S4.**  $^1\text{H}$  NMR (360 MHz,  $\text{CDCl}_3$ ) spectrum of **3**.

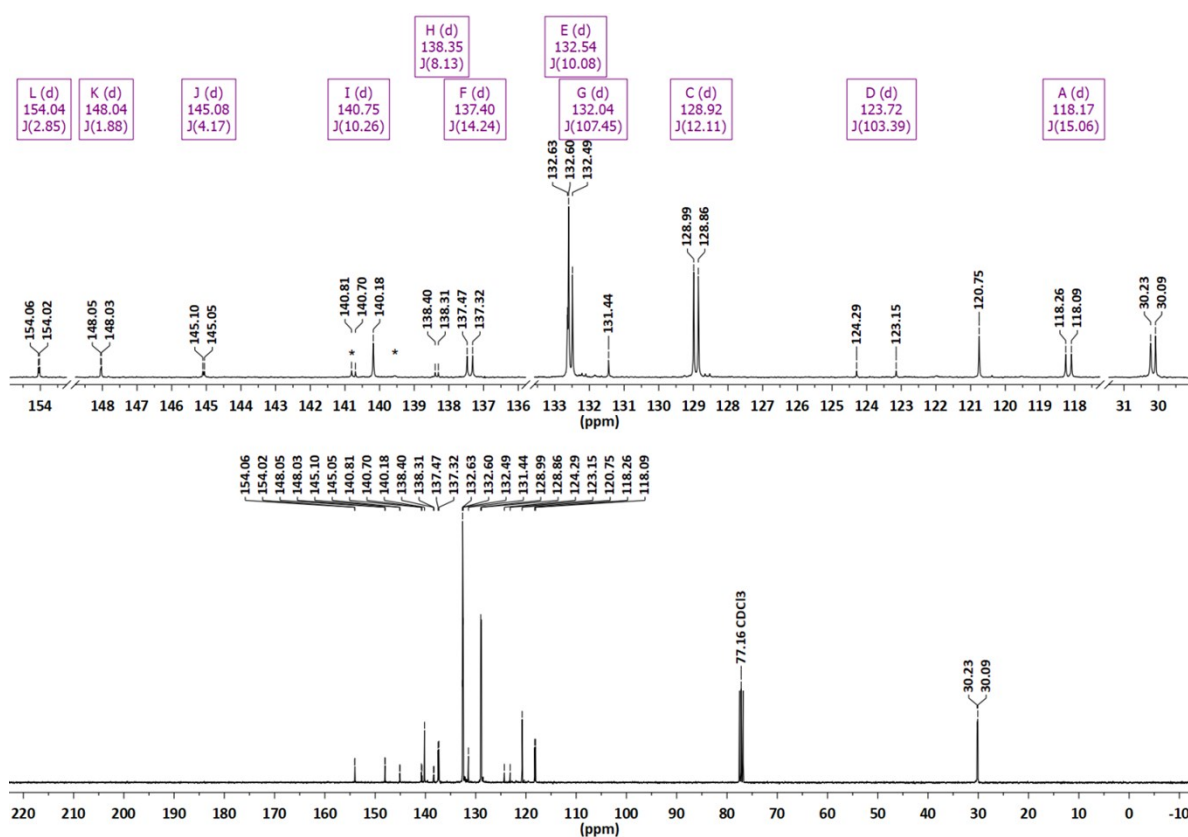


**Figure S5.**  $^{13}\text{C}\{^1\text{H}\}$  NMR (91 MHz,  $\text{CDCl}_3$ ) spectrum of **3** (\* denotes  $^{199}\text{Hg}$  satellites).

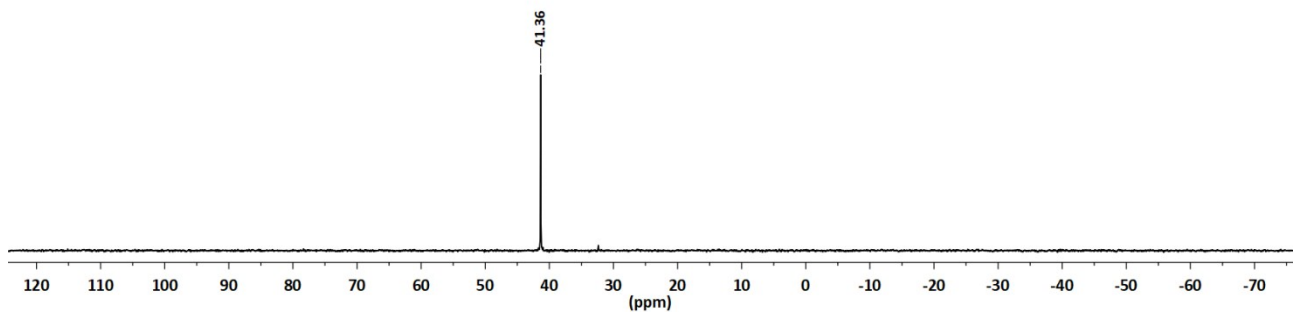


**Figure S6.**  $^{31}\text{P}\{\text{H}\}$  NMR (146 MHz,  $\text{CDCl}_3$ ) spectrum of **3**.

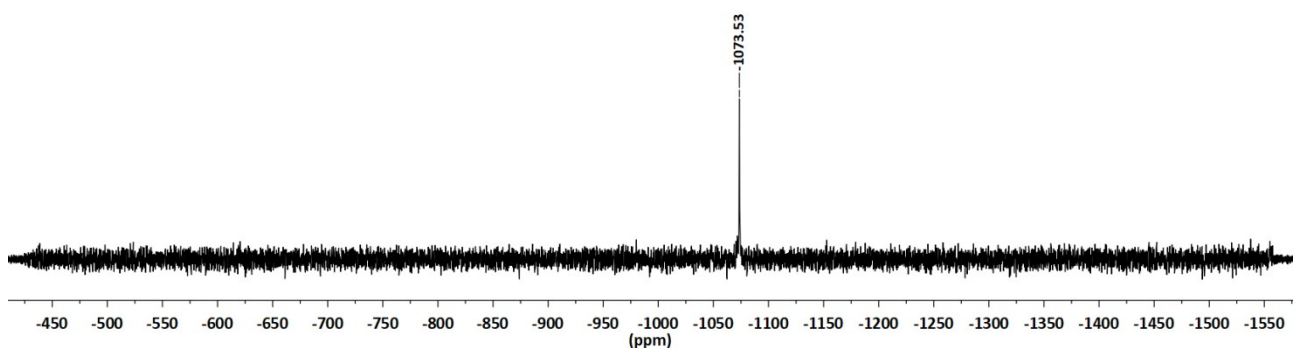


**Figure S7.**  $^{199}\text{Hg}\{\text{H}\}$  NMR (65 MHz,  $\text{CDCl}_3$ ) spectrum of **3**.

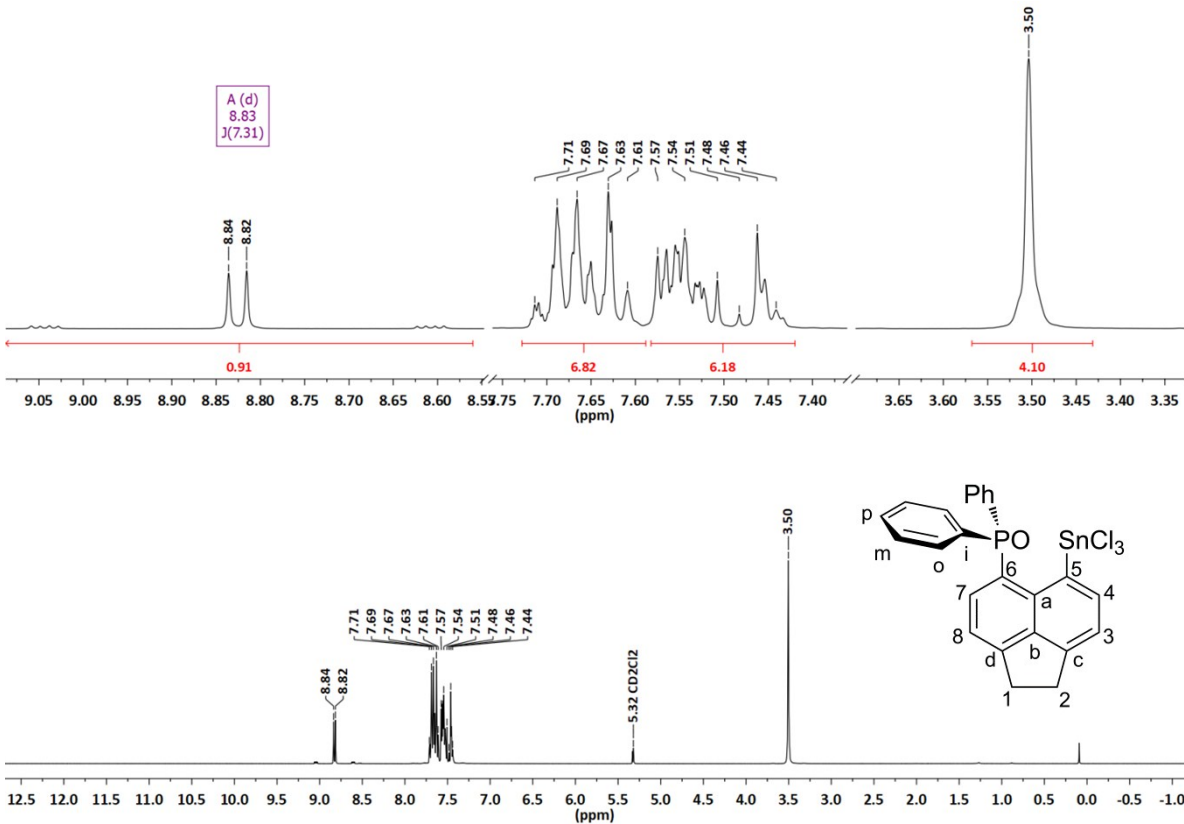


**Figure S8.**  $^1\text{H}$  NMR (360 MHz,  $\text{CD}_2\text{Cl}_2$ ) spectrum of **4**.

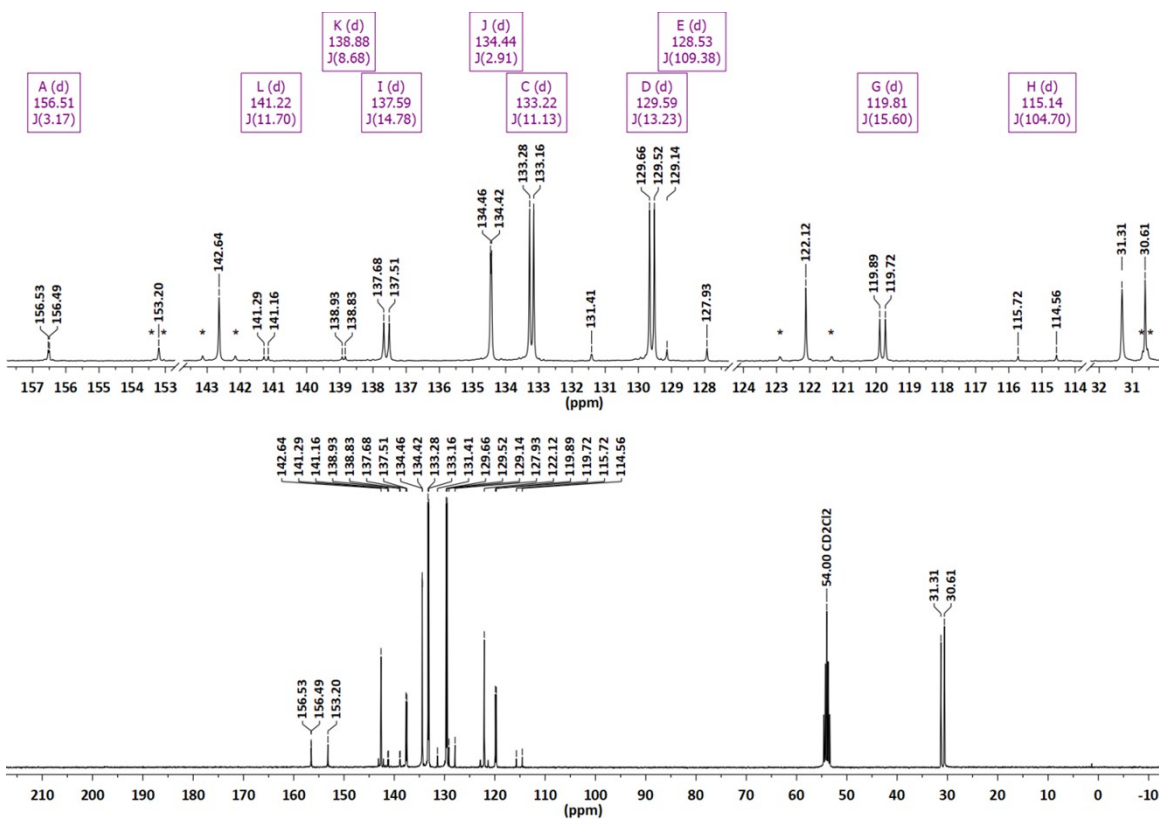


**Figure S9.**  $^{13}\text{C}\{^1\text{H}\}$  NMR (91 MHz,  $\text{CD}_2\text{Cl}_2$ ) spectrum of **4** (\* denotes  $^{119}\text{Sn}$  satellites).

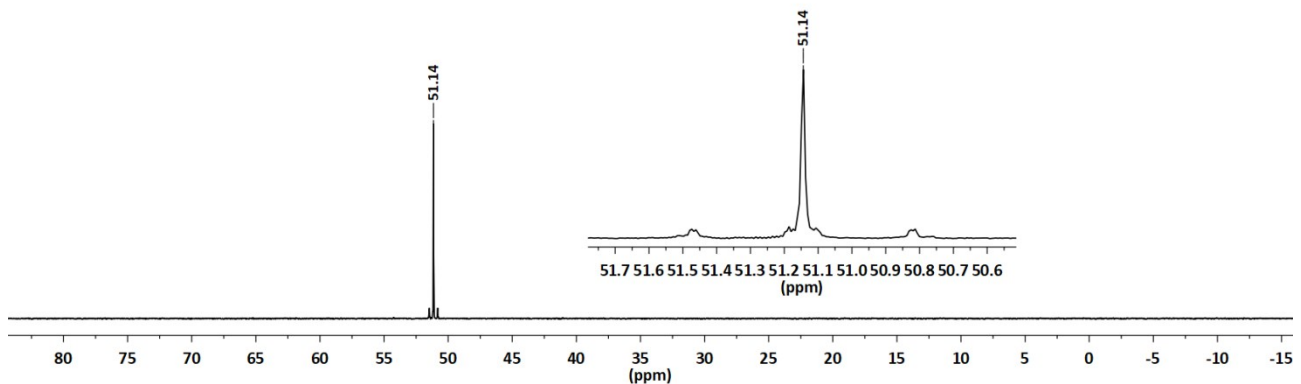


**Figure S10.**  $^{31}\text{P}\{\text{H}\}$  NMR (146 MHz,  $\text{CD}_2\text{Cl}_2$ ) spectrum of **4**.

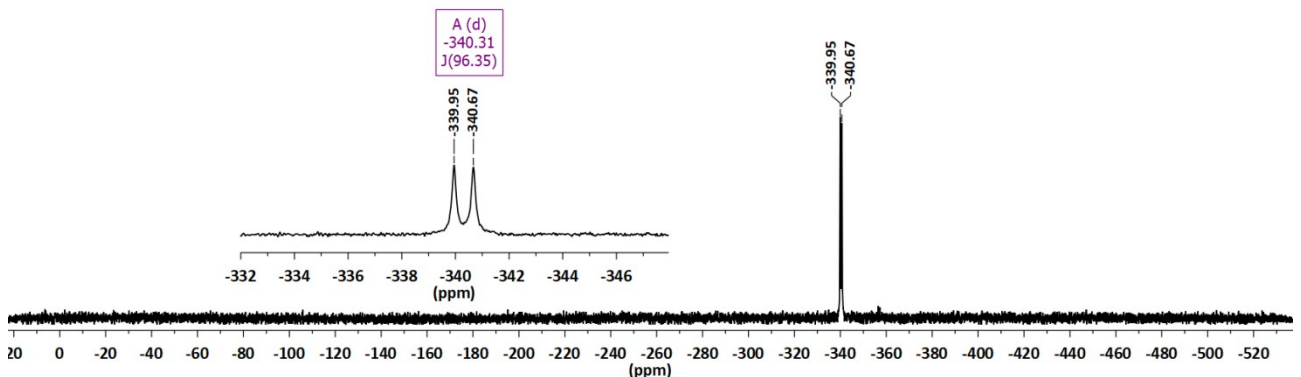


**Figure S11.**  $^{119}\text{Sn}\{\text{H}\}$  NMR (134 MHz,  $\text{CD}_2\text{Cl}_2$ ) spectrum of **4**.

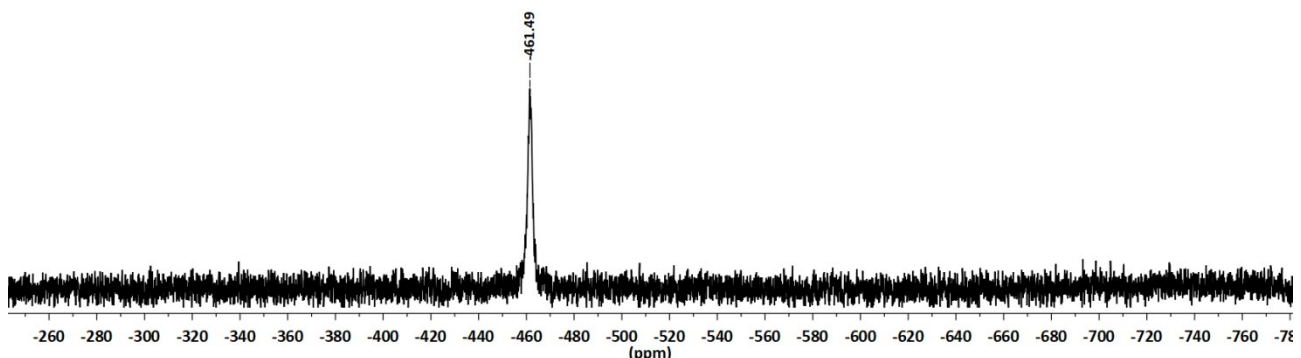


**Figure S12.**  $^{119}\text{Sn}\{\text{H}\}$  NMR (134 MHz,  $\text{CD}_2\text{Cl}_2 + \text{THF}$  ca. 10:1, v/v) spectrum of **4·THF**.

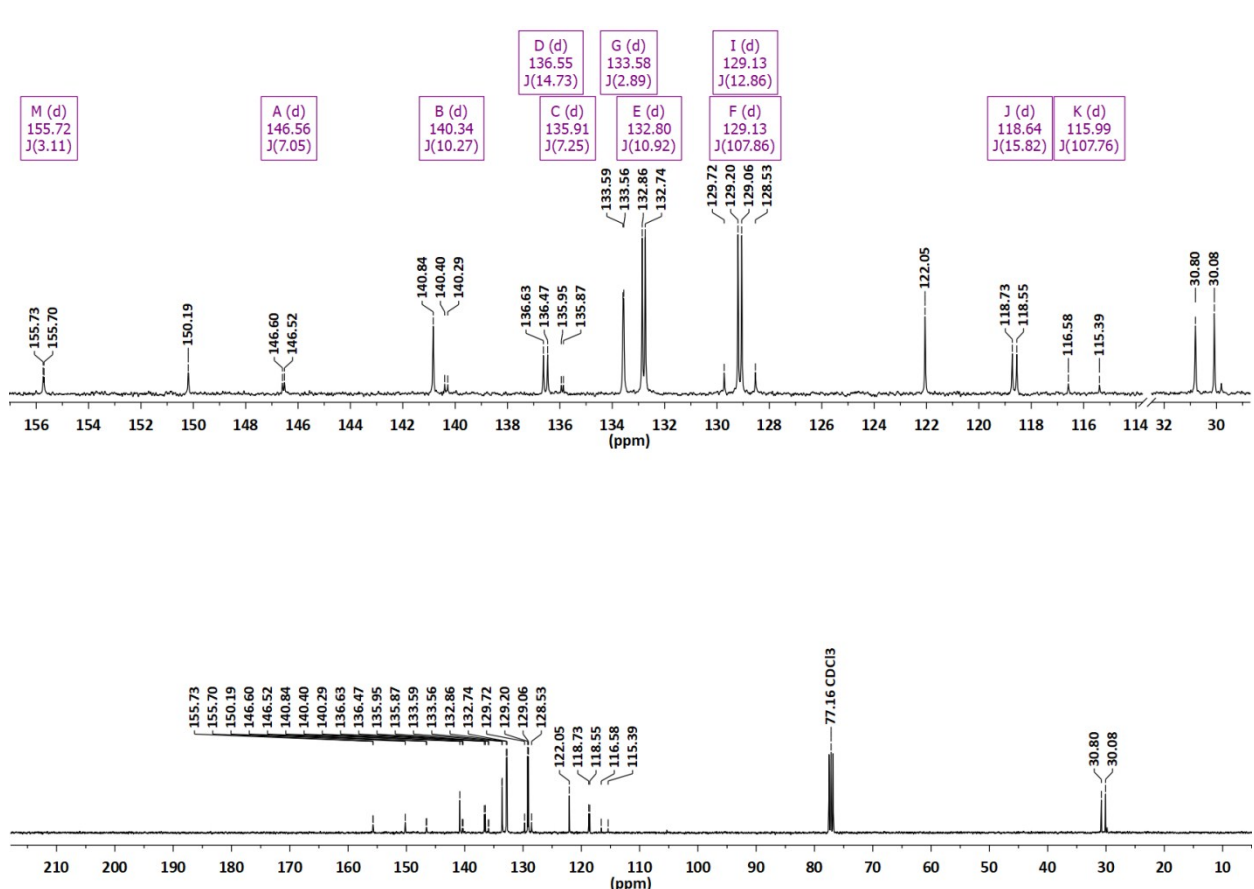
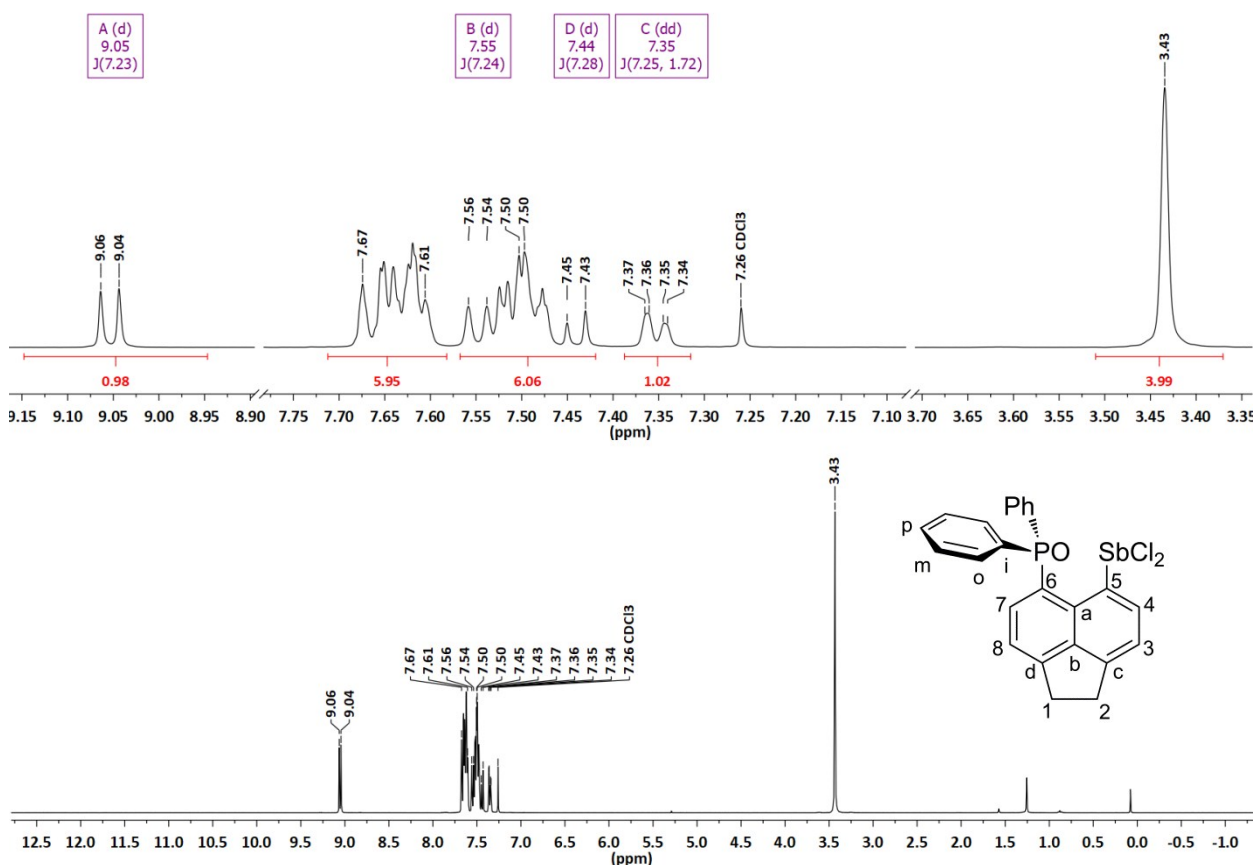


**Figure S14.**  $^{13}\text{C}\{^1\text{H}\}$  NMR (91 MHz,  $\text{CDCl}_3$ ) spectrum of **5**.

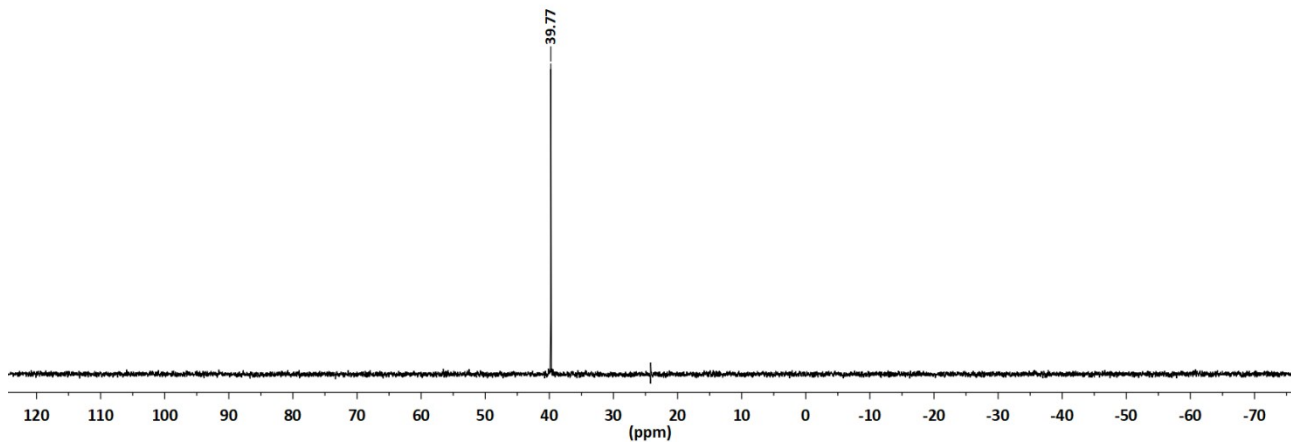


**Figure S15.**  $^{31}\text{P}\{\text{H}\}$  NMR (146 MHz,  $\text{CDCl}_3$ ) spectrum of **5**.

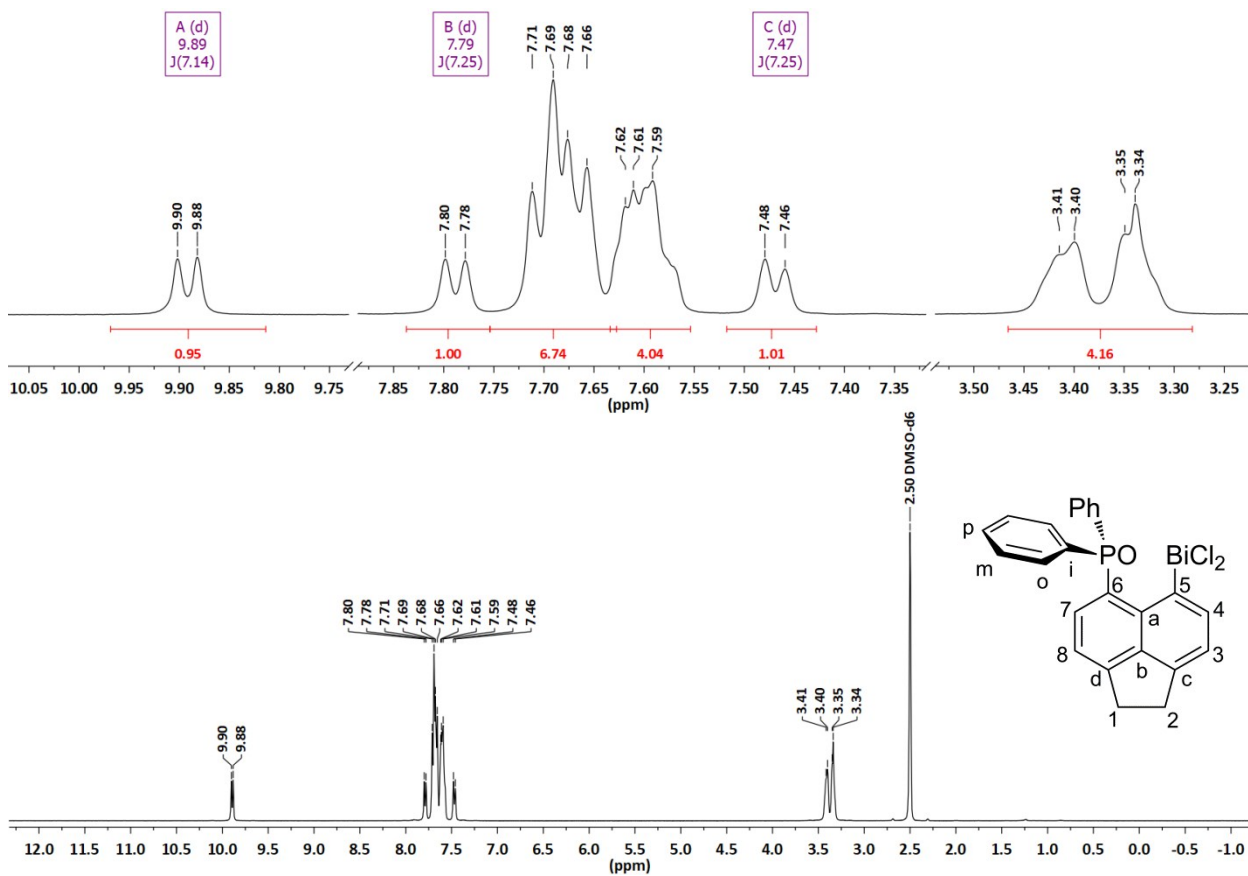


**Figure S16.**  $^1\text{H}$  NMR (360 MHz, DMSO-*d*6) spectrum of **6**.

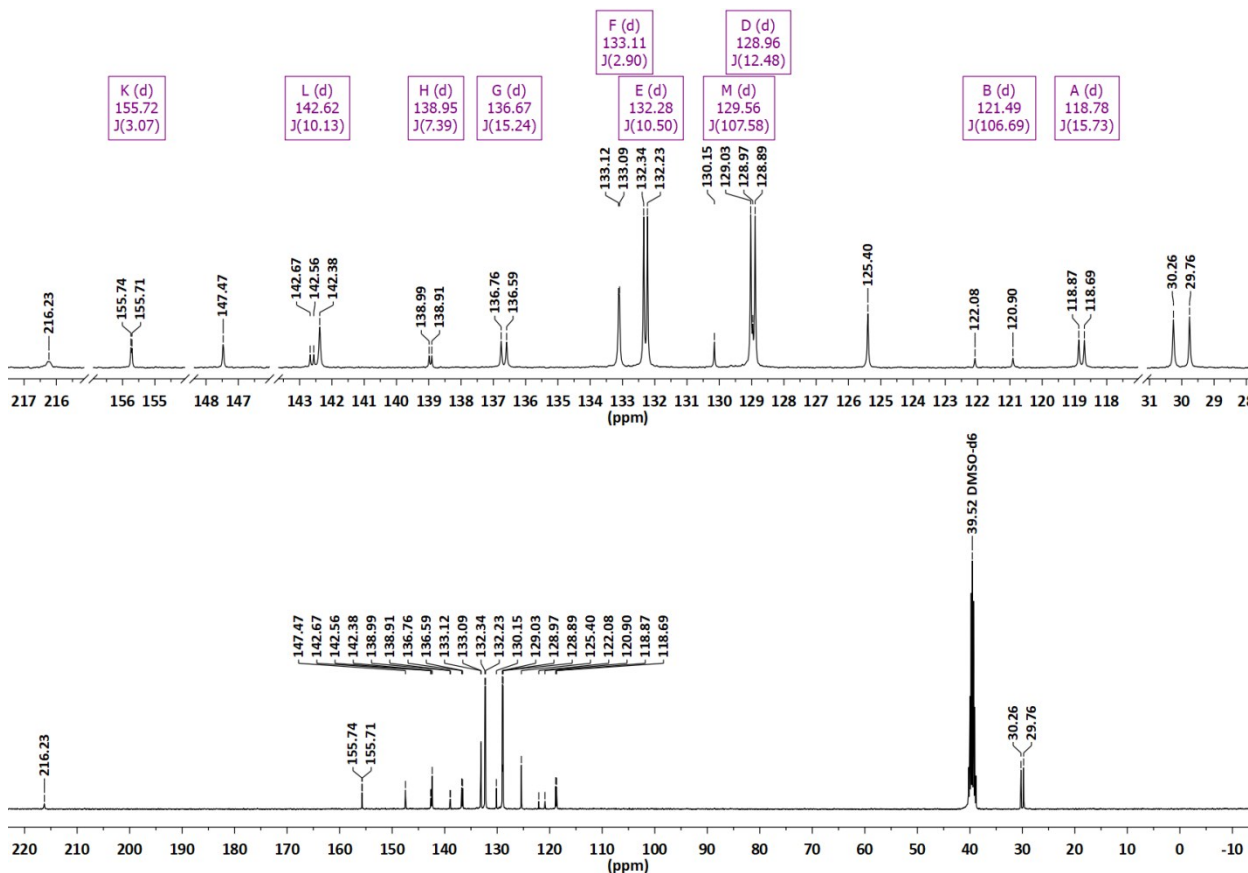


**Figure S17.**  $^{13}\text{C}\{^1\text{H}\}$  NMR (91 MHz, DMSO-*d*6) spectrum of **6**.

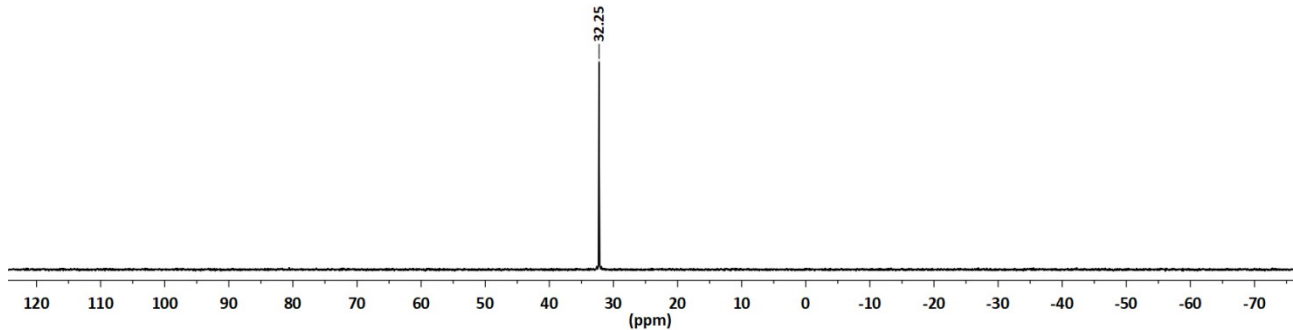


**Figure S18.**  $^{31}\text{P}\{\text{H}\}$  NMR (146 MHz, DMSO-*d*6) spectrum of **6**.

## Computational data

**Table S1.** Topological and integrated bond properties from AIM and ELI-D.

	contact	d [Å]	$\rho(\mathbf{r})$ [eÅ <sup>-3</sup> ]	$\nabla^2\rho(\mathbf{r})$ [eÅ <sup>-5</sup> ]	$\epsilon$	G/ $\rho(\mathbf{r})$ [a.u.]	H/ $\rho(\mathbf{r})$ [a.u.]	N <sub>ELI</sub> [e]	V <sub>ELI</sub> [Å <sup>3</sup> ]	$\gamma_{ELI}$	$\gamma_{ELI'}$
<b>3</b>	PO	1.498	1.59	26.9	0.01	2.11	-0.93	1.60	2.0	1.45	
<b>5</b> ·THF	PO	1.508	1.55	25.2	0.04	2.05	-0.91	1.54	1.9	1.47	
<b>6</b> ·THF	PO	1.509	1.55	25.2	0.01	2.05	-0.91	1.54	1.8	1.47	
<b>5</b>	PO	1.510	1.55	25.1	0.02	2.05	-0.92	1.56	1.9	1.46	
<b>4</b> ·THF	PO	1.513	1.53	24.7	0.03	2.04	-0.90	1.51	1.7	1.48	
<b>6</b>	PO	1.513	1.54	24.7	0.01	2.04	-0.91	1.55	1.8	1.47	
<b>4</b>	PO	1.514	1.52	24.6	0.03	2.03	-0.90	1.49	1.7	1.47	
<b>all</b>	<b>PO</b>	<b>1.509</b>	<b>1.55</b>	<b>25.2</b>	<b>0.02</b>	<b>2.05</b>	<b>-0.91</b>	<b>1.54</b>	<b>1.84</b>	<b>1.47</b>	
<b>3</b>	HgC	2.076	0.89	2.7	0.04	0.68	-0.46	1.88	6.9	1.62	
<b>4</b>	SnC	2.164	0.70	2.2	0.10	0.65	-0.42	2.33	11.1	1.74	
<b>4</b> ·THF	SnC	2.184	0.68	2.1	0.07	0.63	-0.42	2.23	8.3	1.77	
<b>5</b> ·THF	SbC	2.204	0.71	0.6	0.06	0.53	-0.47	2.33	8.1	1.78	
<b>5</b>	SbC	2.209	0.70	0.7	0.07	0.53	-0.46	2.31	8.6	1.77	
<b>6</b> ·THF	BiC	2.300	0.64	1.3	0.07	0.54	-0.39	2.13	8.6	1.74	
<b>6</b>	BiC	2.308	0.63	1.3	0.08	0.53	-0.39	2.13	9.0	1.73	
<b>all</b>	<b>EC</b>	<b>2.206</b>	<b>0.71</b>	<b>1.6</b>	<b>0.07</b>	<b>0.58</b>	<b>-0.43</b>	<b>2.19</b>	<b>8.7</b>	<b>1.74</b>	
<b>4</b> ·THF	SnO1	2.198	0.44	6.4	0.01	1.12	-0.11	6.22	15.9	1.62	
<b>4</b>	SnO1	2.215	0.43	6.1	0.01	1.10	-0.11	5.50	14.6	1.62	
<b>sum</b>	<b>SnO</b>	<b>2.207</b>	<b>0.43</b>	<b>6.2</b>	<b>0.01</b>	<b>1.11</b>	<b>-0.11</b>	<b>6.22</b>	<b>15.7</b>	<b>1.62</b>	<b>1.54</b>
<b>5</b> ·THF	SbO1	2.413	0.32	3.0	0.06	0.77	-0.11	6.14	16.8	1.62	
<b>6</b> ·THF	BiO1	2.444	0.32	3.9	0.02	0.90	-0.05	6.15	17.5	1.61	
<b>5</b>	SbO1	2.446	0.30	2.8	0.04	0.75	-0.11	6.12	16.9	1.61	
<b>6</b>	BiO1	2.464	0.31	3.8	0.01	0.88	-0.04	6.13	17.5	1.61	
<b>sum</b>	<b>Sb/Bi-O</b>	<b>2.442</b>	<b>0.31</b>	<b>3.4</b>	<b>0.03</b>	<b>0.83</b>	<b>-0.08</b>	<b>6.13</b>	<b>17.2</b>	<b>1.61</b>	
<b>3</b>	HgO	2.626	0.22	2.9	0.12	0.92	0.02	6.11	18.2	1.60	
<b>4</b> ·THF	SnO2	2.667	0.17	1.6	0.08	0.69	-0.03	4.93	11.4	1.75	
<b>6</b> ·THF	BiO2	2.850	0.15	1.5	0.15	0.69	0.02	5.02	12.3	1.74	
<b>5</b> ·THF	SbO2	2.952	0.12	1.0	0.01	0.60	-0.01	4.99	12.4	1.74	

For all bonds,  $\rho(\mathbf{r})_{bcp}$  is the electron density at the bond critical point,  $\nabla^2\rho(\mathbf{r})_{bcp}$  is the corresponding Laplacian,  $\epsilon$  is the bond ellipticity, G/ $\rho(\mathbf{r})_{bcp}$  and H/ $\rho(\mathbf{r})_{bcp}$  are the kinetic and total energy density over  $\rho(\mathbf{r})_{bcp}$  ratios, N<sub>ELI</sub> and V<sub>ELI</sub> are electron populations and volumes of related ELI-D basins,  $\gamma_{ELI}$  is the ELI-D value at the attractor position, no. refers to the number of averaged bonds. E = Sn, Sb, Hg, Bi. O<sub>2</sub> = O<sub>THF</sub>.

**Table S2.** Topological and integrated bond properties from AIM and ELI-D.

	contact	d [Å]	$\rho(\mathbf{r})$ [eÅ <sup>-3</sup> ]	$\nabla^2\rho(\mathbf{r})$ [eÅ <sup>-5</sup> ]	$\varepsilon$	G/ $\rho(\mathbf{r})$ [a.u.]	H/ $\rho(\mathbf{r})$ [a.u.]	N <sub>ELI</sub> [e]	V <sub>ELI</sub> [Å <sup>3</sup> ]	$\gamma_{ELI}$	$\gamma_{ELI'}$
<b>3</b>	HgCl	2.315	0.68	4.8	0.01	0.85	-0.36	7.58	38.1	1.65	
<b>4</b>	SnCl <sub>3</sub>	2.354	0.58	3.9	0.06	0.81	-0.34	7.76	37.6	1.67	
<b>4</b> ·THF	SnCl <sub>2</sub>	2.355	0.58	3.9	0.07	0.81	-0.34	7.77	37.4	1.67	
<b>4</b> ·THF	SnCl <sub>2</sub>	2.371	0.57	3.5	0.03	0.78	-0.35	7.10	34.4	1.67	
<b>5</b>	SbCl <sub>2</sub>	2.377	0.59	2.5	0.06	0.69	-0.38	7.32	35.9	1.66	1.45
<b>4</b> ·THF	SnCl <sub>2</sub>	2.391	0.53	3.7	0.03	0.80	-0.32	7.22	36.9	1.65	1.43
<b>5</b> ·THF	SbCl <sub>2</sub>	2.401	0.56	2.5	0.05	0.68	-0.37	7.34	36.3	1.65	
<b>4</b>	SnCl <sub>11</sub>	2.408	0.52	3.4	0.01	0.78	-0.32	7.75	36.7	1.65	
<b>4</b> ·THF	SnCl <sub>11</sub>	2.421	0.51	3.3	0.00	0.77	-0.32	7.35	35.7	1.65	
<b>5</b>	SbCl <sub>11</sub>	2.465	0.50	2.3	0.03	0.66	-0.33	7.74	37.0	1.64	
<b>6</b>	BiCl <sub>2</sub>	2.485	0.52	3.0	0.03	0.71	-0.30	7.62	37.6	1.65	
<b>5</b> ·THF	SbCl <sub>11</sub>	2.495	0.47	2.1	0.04	0.63	-0.32	7.76	36.6	1.63	
<b>5</b> ·THF	BiCl <sub>2</sub>	2.532	0.47	2.9	0.05	0.69	-0.27	7.63	37.8	1.64	
<b>6</b>	BiCl <sub>11</sub>	2.568	0.44	2.9	0.02	0.71	-0.25	7.61	37.9	1.62	
<b>5</b> ·THF	BiCl <sub>11</sub>	2.592	0.42	2.8	0.03	0.70	-0.24	7.63	37.7	1.62	
<b>all</b>	ECl	<b>2.435</b>	<b>0.53</b>	<b>3.2</b>	<b>0.03</b>	<b>0.74</b>	<b>-0.32</b>	<b>7.71</b>	<b>37.2</b>	<b>1.65</b>	<b>1.45</b>
<b>5</b>	LP(Sb)							2.21	18.6	1.93	
<b>5</b> ·THF	LP(Sb)							2.16	16.7	1.96	
<b>6</b>	LP(Bi)							1.93	16.9	1.53	
<b>6</b> ·THF	LP(Bi)							1.69	13.6	1.56	

For all bonds,  $\rho(\mathbf{r})_{bcp}$  is the electron density at the bond critical point,  $\nabla^2\rho(\mathbf{r})_{bcp}$  is the corresponding Laplacian,  $\varepsilon$  is the bond ellipticity, G/ $\rho(\mathbf{r})_{bcp}$  and H/ $\rho(\mathbf{r})_{bcp}$  are the kinetic and total energy density over  $\rho(\mathbf{r})_{bcp}$  ratios, N<sub>ELI</sub> and V<sub>ELI</sub> are electron populations and volumes of related ELI-D basins,  $\gamma_{ELI}$  is the ELI-D value at the attractor position, no. refers to the number of averaged bonds. E = Sn, Sb, Hg, Bi.

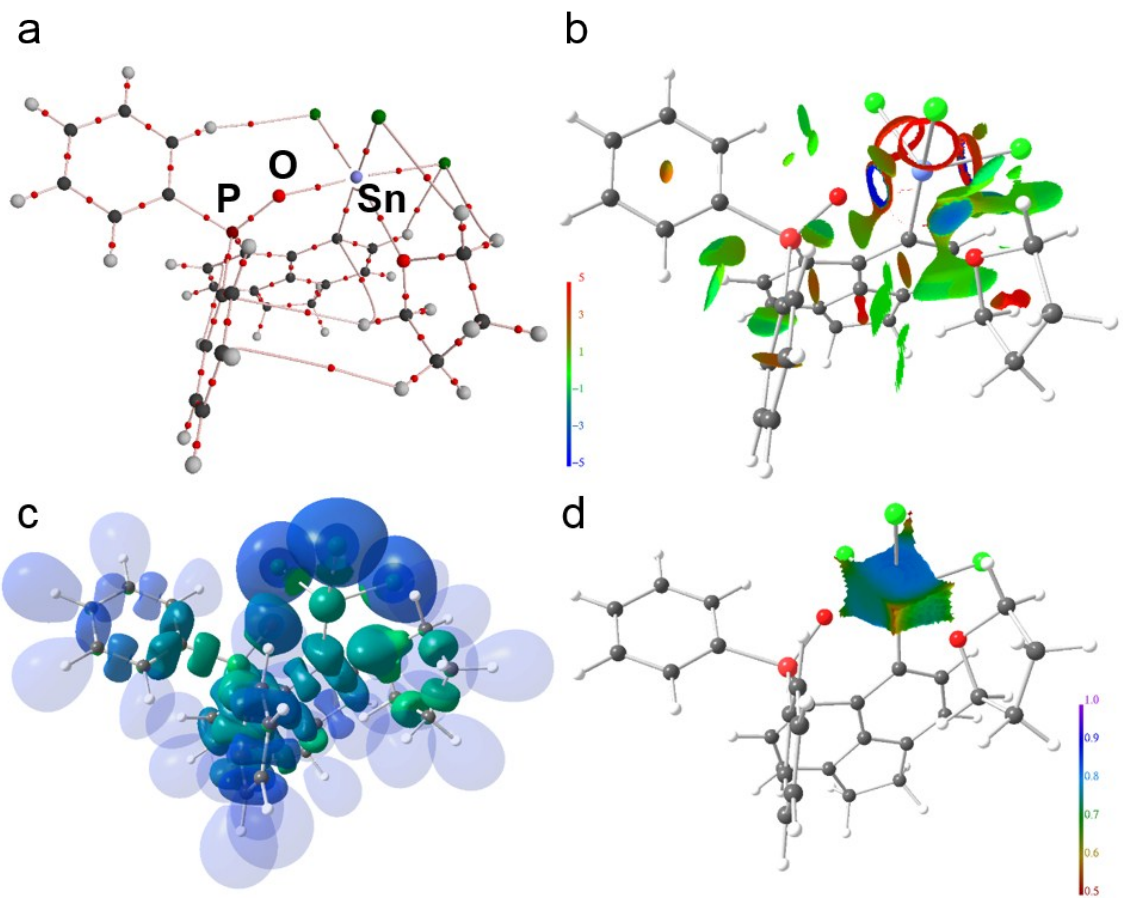


**Figure S19.** RSBI analysis of  $4 \cdot$ THF. (a) AIM bond paths motif, (b) NCI *iso*-surface at  $s(r) = 0.5$ , (c) ELI-D localization domain representation at *iso*-value of 1.3, (d) ELI-D distribution mapped on the Sn–P ELI-D basin.

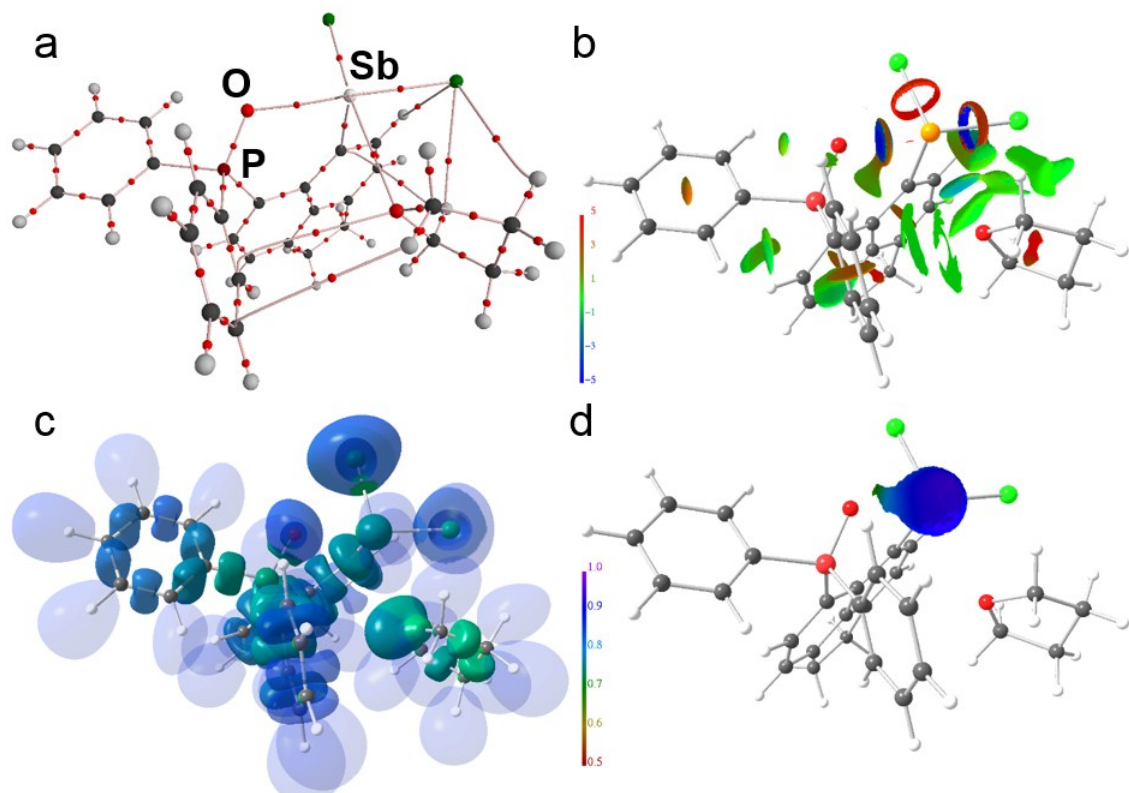


**Figure S20.** RSBI analysis of **5**·THF (a) AIM bond paths motif, (b) NCI *iso*-surface at  $s(\mathbf{r}) = 0.5$ , (c) ELI-D localization domain representation at *iso*-value of 1.3, (d) ELI-D distribution mapped on the Sn–P ELI-D basin.

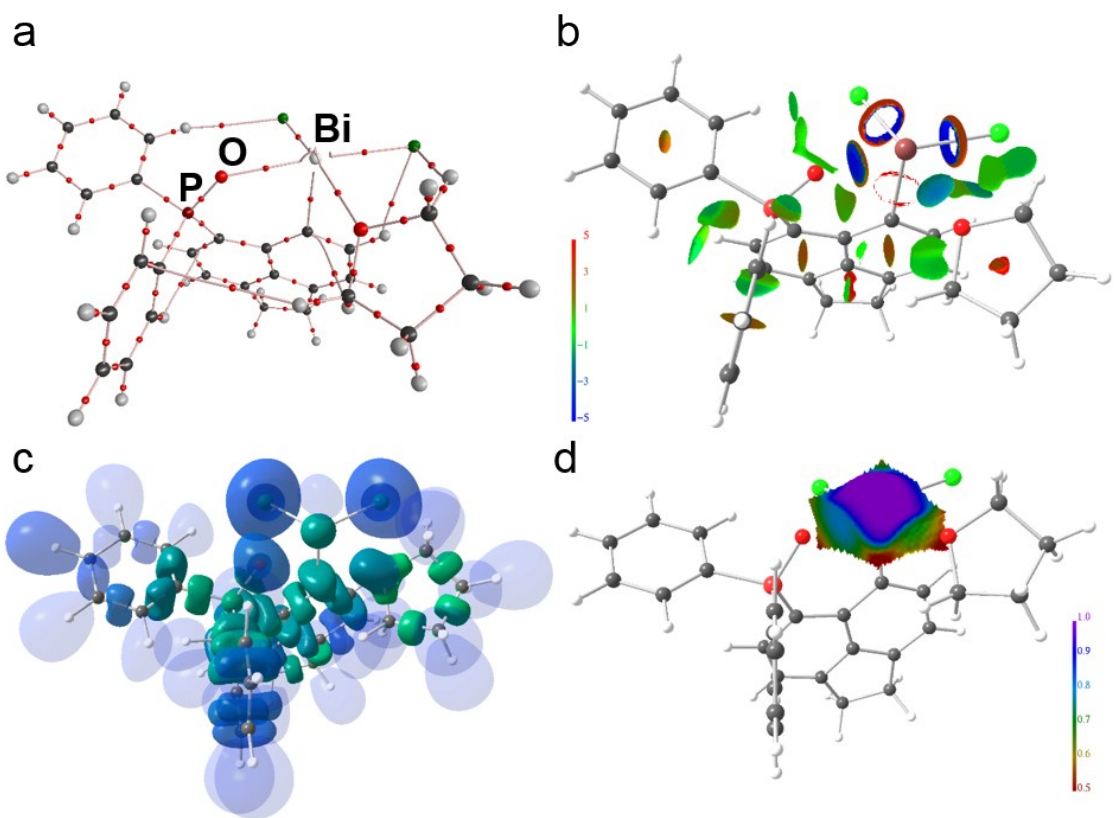


**Figure S21.** RSBI analysis of **6**·THF (a) AIM bond paths motif, (b) NCI *iso*-surface at  $s(\mathbf{r}) = 0.5$ , (c) ELI-D localization domain representation at *iso*-value of 1.3, (d) ELI-D distribution mapped on the Sn–P ELI-D basin.

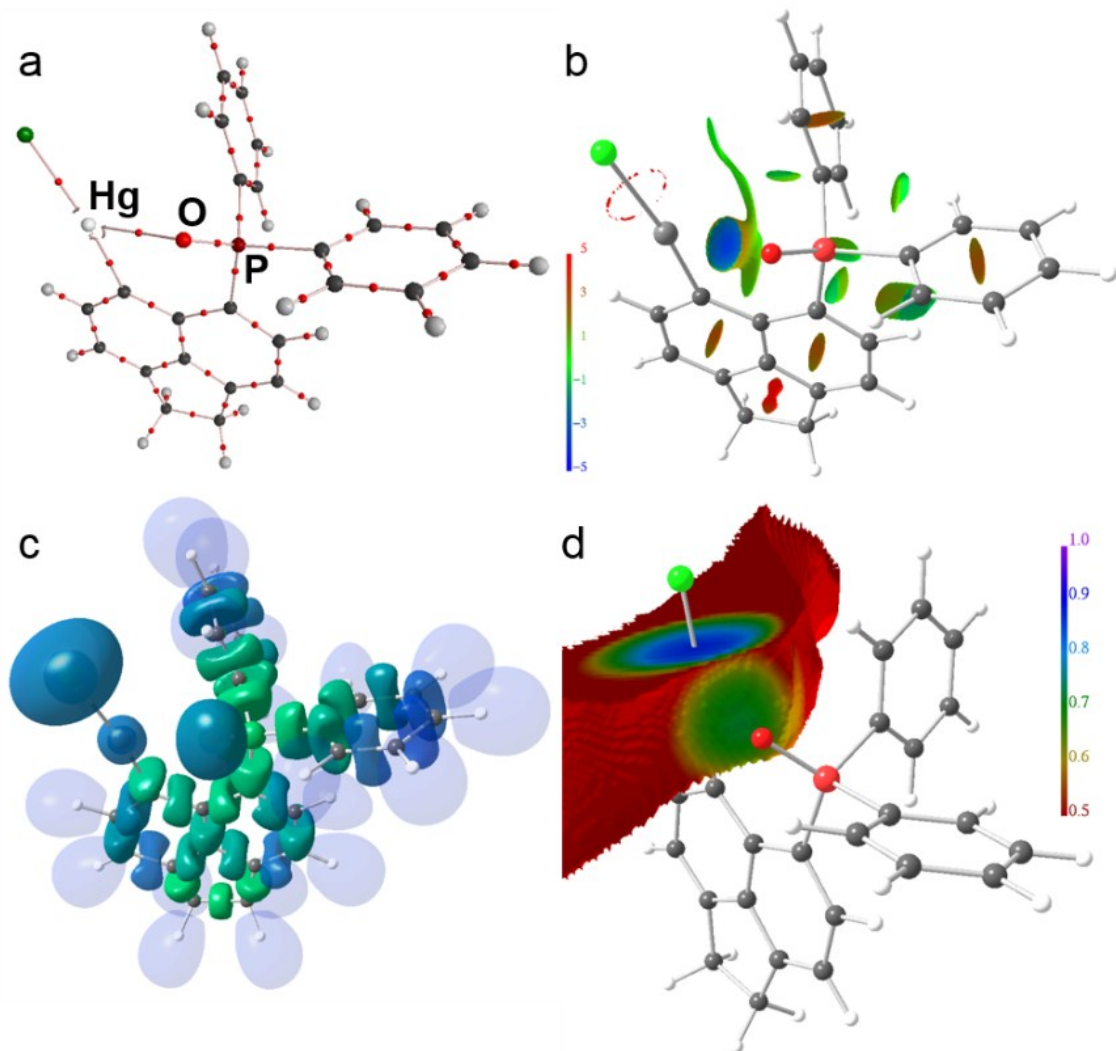


**Figure S22** RSBI analysis of **3**. (a) AIM bond paths motif, (b) NCI *iso*-surface at  $s(\mathbf{r}) = 0.5$ , (c) ELI-D localization domain representation at *iso*-value of 1.3, (d) ELI-D distribution mapped on the Sn–P ELI-D basin.

## Crystallographic data

**Table S3.** Crystal data and structure refinement

	<b>1a·2CH<sub>2</sub>Cl<sub>2</sub></b>	<b>3·THF</b>	<b>4</b>
Formula	C <sub>98</sub> H <sub>76</sub> Cl <sub>5</sub> Hg <sub>2</sub> LiO <sub>4</sub> P <sub>4</sub>	C <sub>24</sub> H <sub>18</sub> ClHgOP	C <sub>24</sub> H <sub>18</sub> Cl <sub>3</sub> OPSn
Formula weight, g mol <sup>-1</sup>	2026.84	589.39	578.39
Crystal system	Triclinic	Monoclinic	Triclinic
Crystal size, mm	0.08 × 0.08 × 0.08	0.07 × 0.05 × 0.05	0.06 × 0.05 × 0.04
Space group	P <sup>1</sup>	P2 <sub>1</sub> /n	P <sup>1</sup>
<i>a</i> , Å	14.2748(8)	10.8014(4)	8.9934(4)
<i>b</i> , Å	15.6725(8)	10.3777(4)	9.5252(4)
<i>c</i> , Å	21.2164(11)	18.5406(8)	14.9658(6)
$\alpha$ , °	105.246(2)	90	102.200(1)
$\beta$ , °	98.704(2)	105.655(1)	98.392(1)
$\gamma$ , °	94.464(2)	90	113.284(1)
<i>V</i> , Å <sup>3</sup>	4492.2(4)	2001.2(1)	1112.79(8)
<i>Z</i>	2	4	2
$\rho_{\text{calcd}}$ , Mg m <sup>-3</sup>	1.498	1.956	1.726
$\mu$ (Mo $K\alpha$ ), mm <sup>-1</sup>	3.684	7.917	1.595
<i>F</i> (000)	2008	1128	572
$\theta$ range, deg	2.60 to 28.28	2.27 to 30.57	2.44 to 31.61
Index ranges	$-19 \leq h \leq 19$ $-20 \leq k \leq 20$ $-28 \leq l \leq 25$	$-15 \leq h \leq 15$ $-14 \leq k \leq 14$ $-26 \leq l \leq 26$	$-13 \leq h \leq 13$ $-13 \leq k \leq 14$ $-22 \leq l \leq 22$
No. of reflns collected	126062	76418	43017
Completeness to $\theta_{\text{max}}$	99.9%	99.8%	99.4%
No. indep. Reflns	22272	6128	7411
No. obsd reflns with( $I > 2\sigma(I)$ )	18428	5850	6826
No. refined params	1027	253	271
GooF ( $F^2$ )	1.078	1.176	1.062
$R_1(F)$ ( $I > 2\sigma(I)$ )	0.0544	0.0198	0.0246
$wR_2(F^2)$ (all data)	0.1216	0.0516	0.0573
Largest diff peak/hole, e Å <sup>-3</sup>	4.052 / -3.526	0.651 / -2.109	0.636 / -1.399
CCDC number	1897901	1897902	1897903

**Table S3.** cont

<b>4</b> ·THF	<b>5</b>	<b>5</b> ·THF	<b>6</b>
C <sub>32</sub> H <sub>34</sub> Cl <sub>3</sub> O <sub>3</sub> PSn	C <sub>24</sub> H <sub>18</sub> Cl <sub>2</sub> OPSb	C <sub>28</sub> H <sub>26</sub> Cl <sub>2</sub> O <sub>2</sub> PSb	C <sub>25</sub> H <sub>20</sub> BiCl <sub>4</sub> OP
722.60	546.00	618.11	718.16
Triclinic	Monoclinic	Triclinic	Triclinic
0.08 × 0.06 × 0.04	0.07 × 0.06 × 0.04	0.08 × 0.07 × 0.07	0.08 × 0.07 × 0.05
P $\bar{1}$	P2 <sub>1</sub> /n	P $\bar{1}$	P $\bar{1}$
8.8921(3)	8.6794(3)	9.2077(3)	9.1561(3)
10.4750(4)	12.6557(5)	9.6481(4)	11.7354(4)
16.9858(7)	19.5559(8)	15.3566(6)	12.0175(5)
85.291(1)	90	97.547(1)	90.800(1)
84.161(1)	97.497(1)	97.893(1)	105.168(1)
72.333(1)	90	110.393(1)	95.897(1)
1497.5(1)	2129.73(14)	1242.80(8)	1238.58(8)
2	4	2	2
1.603	1.703	1.652	1.926
1.207	1.635	1.414	7.630
732	1080	620	688
2.32 to 30.58	2.28 to 28.35	2.30 to 28.42	2.32 to 35.63
-12 ≤ h ≤ 12	-12 ≤ h ≤ 12	-12 ≤ h ≤ 11	-15 ≤ h ≤ 15
-14 ≤ k ≤ 14	-17 ≤ k ≤ 18	-12 ≤ k ≤ 12	-19 ≤ k ≤ 19
-24 ≤ l ≤ 24	-27 ≤ l ≤ 27	-20 ≤ l ≤ 20	-19 ≤ l ≤ 18
48875	98732	73343	63344
99.6%	99.8%	99.2%	99.9%
9171	6549	6215	11415
8229	6038	5770	10581
361	262	307	289
1.068	1.244	1.064	1.126
0.0257	0.0214	0.0233	0.0247
0.0546	0.0610	0.0589	0.0577
0.740 / -0.801	0.559 / -1.204	0.567 / -1.294	2.568 / -3.007
1897904	1897905	1897906	1897907